Visualizing the Limitations of Four-State Measurement of PDL and Results of a Six-State Alternative

R. M. Craig
Optoelectronics Division
Electronics and Electrical Engineering Laboratory
National Institute of Standards and Technology
Boulder, CO 80305

Abstract

I present a method of visualizing polarization-dependent loss in single-mode optical fiber and components. This method uses generalized Poincaré spheroids wherein the power (though polarized) is no longer normalized to unity. The resulting graphical development permits a better understanding of the limitations of the four-state Mueller-Stokes measurement of this parameter in the presence of combined parasitic birefringence and external polarization-dependent losses. A six-state alternative that improves accuracy and repeatability is shown along with the results of preliminary comparative measurements. The alternative is also found to be more tolerant of non-orthogonal states while maintaining short measurement times.

Introduction

The widespread use of wavelength multiplexing necessitates the rapid measurement of polarization-dependent loss (PDL) over wavelength, which I refer to as PDL_λ. Currently, PDL_λ is typically measured with either a random all-states (A/S) technique [1] or the four-state technique of Nyman, et al.[2,3] which I refer to as Mueller-Stokes (M/S). The all-states technique is precise and simple to apply, but typically slow for wavelength-dependent measurements. However, the A/S method is only as accurate as the statistical sum of all internal system PDL's [4]. By contrast, the four-state M/S method is typically very fast and capable of subtracting the effect of internal system PDL, which makes it potentially much more accurate in a laboratory setting. However, in field or production situations, conditions can be far from ideal, with large parasitic birefringence and PDL sources in the optical circuit. In addition, the M/S technique assumes strict orthogonality of the polarized states wherein the four states are separated by equal quadrants on the Poincaré sphere [5]. When this condition is not met, the M/S method can show dramatic uncertainties that serve to negate much of the perceived benefits. Long, coiled and unrestrained patch cords can lead to large values of static and dynamic strain birefringence [6]. Poor connectors and open beams can lead to large parasitic PDL in the circuit, while misalignment or wavelength dependence in the polarization controller can lead to non-orthogonality of input states. Though not always present, the combination of these effects can be devastating to the accuracy of the M/S method. My goal has been to understand the nature of this limitation and to devise a suitable alternative that retains the speed benefit while reducing the impact of parasitic effects.

Visualizing PDL

To visualize PDL and its interactions, it is useful to consider Poincaré spheroids: a unit intensity (radius) sphere representing the input polarization state, and an output spheroid of polarization-dependent intensity. A computer model produces the viewpoint seen in Fig. 1 for the example of a 3 dB PDL, where the distorted output spheroid (PDL) is coincident within the unit input sphere. Relative to the input reference frame, the output spheroid can appear "rotated" if the PDL is seen through a retarder (middle image). Adding two orthogonal 3 dB PDL's is equivalent to multiplying the equivalent spheroids, which overlap along the "PDL axis", to generate a half-unit Poincaré sphere, i.e., a 3 dB attenuator (right image).

With the aid of this device, it is now possible to better understand the limitations of the M/S method by allowing us to see the newly obvious symmetries or lack thereof.

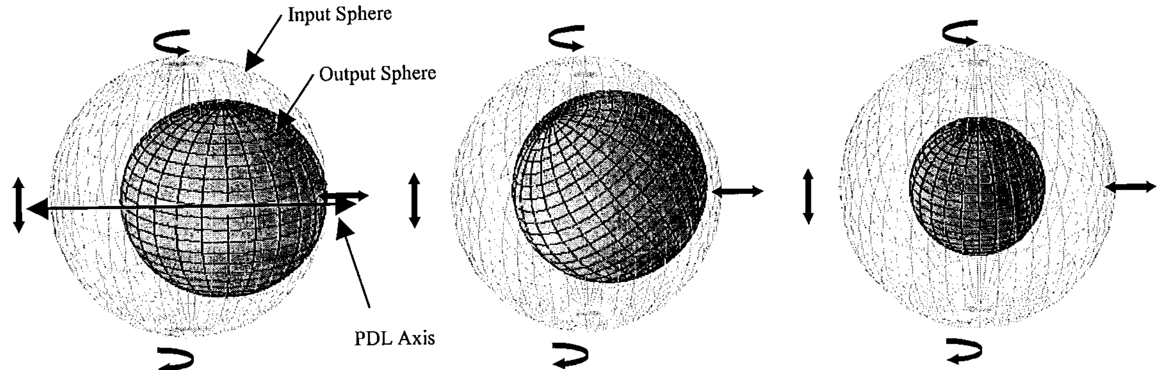

A 3dB PDL following an unpolarized source | A 3dB PDL as seen through a retarder | Result of crossing orthogonal 3dB PDL's

Figure 1: Visualizing a 3 dB PDL and certain interactions with the aid of Poincaré spheroids (inside the unit sphere) that depict the actual Stokes intensity.

The Four-State Problem Viewed Geometrically

The ideal four states of the M/S method can be represented by partial, orthogonal great-circle trajectories, as in Fig. 2. In actual measurements, however, the relative positions of the four states may vary somewhat, particularly with wavelength λ. This variation will lead to non-orthogonal states and a further loss of symmetry. For the purposes of this example, we may take the unit sphere as representing the light as launched from the measurement system and the internal prolate spheroid as representing the light as it exits the device-under-test (DUT). Note that, as long as the axis of any retardance is coincident

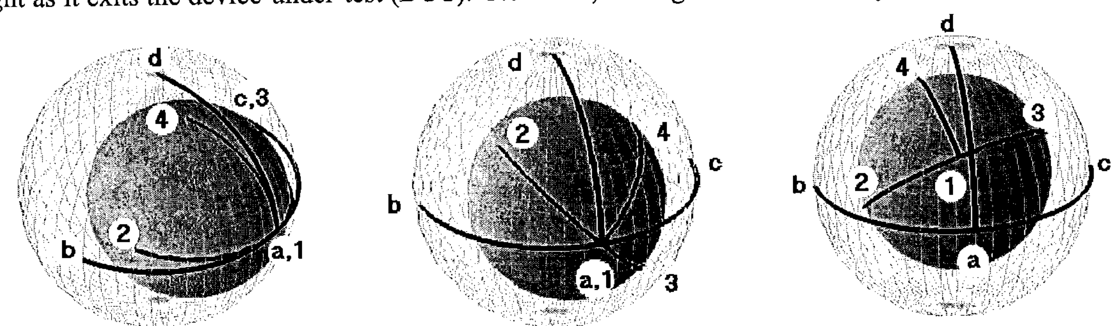

No Parasitic Birefringence | Lead Retardance Axis Coincident with PDL Axis | Lead Retardance Axis Not Coincident with PDL Axis

Figure 2: 4-State M/S trajectories superimposed on the input (system) and output (DUT) spheroids.

with the PDL axis, symmetry is maintained and ratios of relative radii between corresponding system and DUT trajectories (a – 1, b – 2, c – 3, d – 4) are maintained. Conversely, when the parasitic retardance axis is not coincident with the PDL axis, symmetry is broken and the 4-state approach loses information. A simplified M/S measurement system described by this and a later model is shown in Fig. 3.

The Six-State Generalization

Significant improvement is offered by the six-state approach of Fig. 3, which is characterized by the incorporation of additional geometrical information afforded by the greater symmetry available in Poincaré space. The fundamental idea is to require that 4-state measurements about the 1-2-3 plane must be equivalent, i.e., measurements at states 1,2,3,4 or 5,2,3,6. This equivalence is used to generate six equations in six unknown Mueller matrix elements. However four unknowns can be combined into two matrix elements (m_{13} and m_{14}) by taking an average based on symmetry. The result is the comparison table shown below in Table 1, where $m_{11}(\lambda)\ldots m_{14}(\lambda)$ are the Mueller matrix elements relevant to PDL.

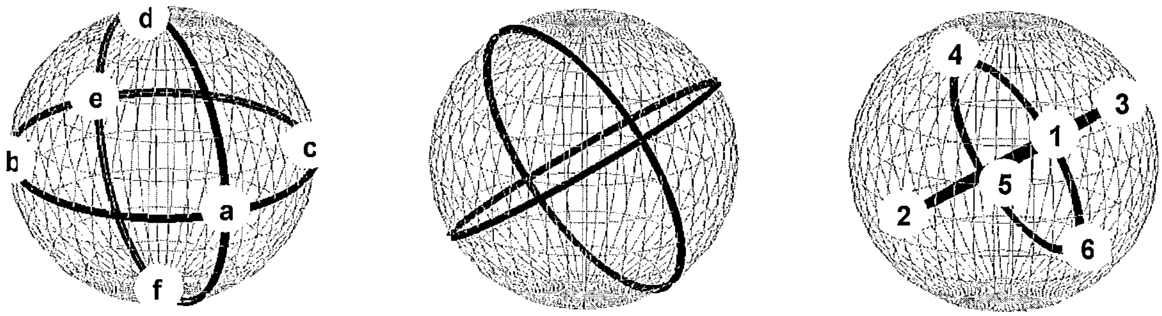

No PDL, No Birefringence | No PDL, Birefringence Present | PDL Present, Birefringence Present

Figure 3: Simplified representation of the polarization state trajectories associated with the 6-state generalization of the M/S technique for both the measurement system and DUT.

The $I_a(\lambda)\ldots I_f(\lambda)$ are measurement system baseline intensities at each input polarization state, while the $I_1(\lambda)\ldots I_6(\lambda)$ are the corresponding intensities when the DUT is in series with parasitic retardances.

Table 1

4-State Matrix Elements

$$\begin{bmatrix} m_{11}(\lambda) \\ m_{12}(\lambda) \\ m_{13}(\lambda) \\ m_{14}(\lambda) \end{bmatrix} = \begin{bmatrix} \frac{1}{2}\left[\frac{I_1(\lambda)I_b(\lambda)+I_2(\lambda)I_a(\lambda)}{I_a(\lambda)I_b(\lambda)}\right] \\ \frac{1}{2}\left[\frac{I_1(\lambda)I_b(\lambda)-I_2(\lambda)I_a(\lambda)}{I_a(\lambda)I_b(\lambda)}\right] \\ -\frac{1}{2}\left[\frac{I_1(\lambda)}{I_a(\lambda)}+\frac{I_2(\lambda)}{I_b(\lambda)}\right]+\frac{I_3(\lambda)}{I_c(\lambda)} \\ -\frac{1}{2}\left[\frac{I_1(\lambda)}{I_a(\lambda)}+\frac{I_2(\lambda)}{I_b(\lambda)}\right]+\frac{I_4(\lambda)}{I_d(\lambda)} \end{bmatrix}$$

6-State Matrix Elements

$$\begin{bmatrix} m_{11}(\lambda) \\ m_{12}(\lambda) \\ m_{13}(\lambda) \\ m_{14}(\lambda) \end{bmatrix} = \begin{bmatrix} \frac{1}{2}\left[\frac{I_1(\lambda)I_b(\lambda)+I_2(\lambda)I_a(\lambda)}{I_a(\lambda)I_b(\lambda)}\right] \\ \frac{1}{2}\left[\frac{I_1(\lambda)I_b(\lambda)-I_2(\lambda)I_a(\lambda)}{I_a(\lambda)I_b(\lambda)}\right] \\ \frac{1}{2}\left[\frac{I_3(\lambda)I_e(\lambda)-I_5(\lambda)I_c(\lambda)}{I_c(\lambda)I_e(\lambda)}\right] \\ \frac{1}{2}\left[\frac{I_4(\lambda)I_f(\lambda)-I_6(\lambda)I_d(\lambda)}{I_d(\lambda)I_f(\lambda)}\right] \end{bmatrix}$$

$$PDL_\lambda \equiv PDL(\lambda) = 10\log\left[\frac{m_{11}(\lambda)+\sqrt{m_{12}(\lambda)^2+m_{13}(\lambda)^2+m_{14}(\lambda)^2}}{m_{11}(\lambda)-\sqrt{m_{12}(\lambda)^2+m_{13}(\lambda)^2+m_{14}(\lambda)^2}}\right] \quad (dB)$$

Results and Conclusion

From the figure and table above, it is clear that for the small additional "expense" of two additional measurements we are gaining considerable symmetrical information that will help to offset the uncertainties associated with parasitic birefringence and other PDL's in the system. The system of Fig. 4 was used to test this approach, and the results of a comparison measurement of a 0.395 dB PDL is presented in Fig. 5. A 0.1 dB PDL artifact was placed in series with the state randomizer (a separate polarization controller) that was stepped through 100 various states following the initial baseline measurement. The 0.1 dB artifact acted as a parasitic PDL in the optical circuit, and the polarization state

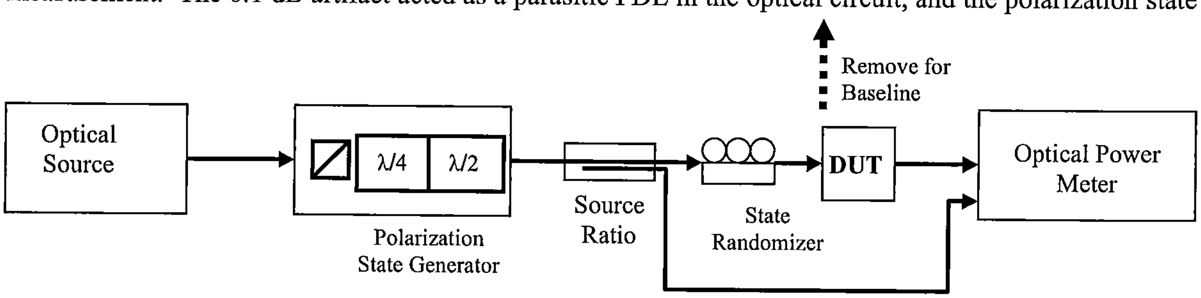

Figure 4: A typical configuration for 4 and 6-state PDL measurements. The randomizer allows for testing system repeatability under various conditions of parasitic birefringence.

randomizer allowed the method to be tested under various polarization conditions, simulating different orientations of parasitic birefringence within the measurement system. The result of these 100

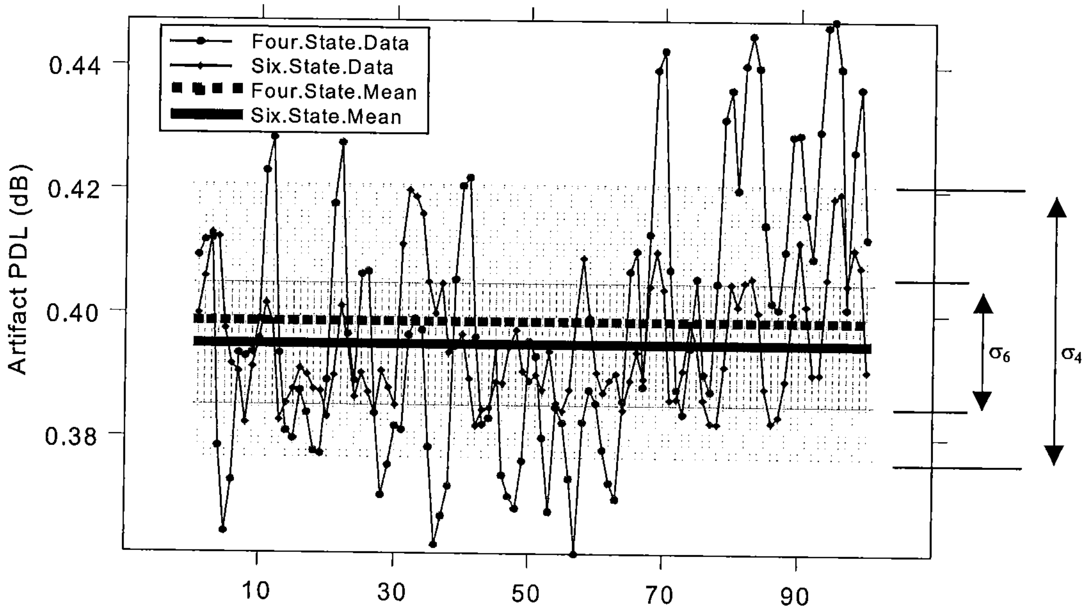

Figure 5: Comparison measurement of a 0.395 dB PDL at 1550 nm using the 4-state and 6-state M/S methods with the apparatus of Fig. 4. Standard deviations are shown at right.

measurements was a clear improvement in both mean and standard deviation for the 6-state method over the 4-state method. The 6-state result was 0.396 ± 0.009 dB while the 4-state result was 0.398 ± 0.021 dB. Though numerical models show that the 6-state method is essentially exact for perfectly orthogonal states, even under parasitic influence, the inclusion of slight non-orthogonality produces some uncertainty. However, for an equivalent deviation from orthogonality in both the 4-state and 6-state methods, the models readily reproduce the approximate factor of two improvement in standard deviation. This method and further generalizations are now being implemented at NIST with the goal of qualifying PDL artifacts to higher accuracy than before.

Bibliography

[1] Derickson, D., *Fiber Optic Test and Measurement* Upper Saddle River, NJ: Prentice Hall PTR, 1998.

[2] Craig, R. M., Gilbert, S. L., and Hale, P. D., "High-resolution, nonmechanical approach to polarization-dependent transmission measurements," *Journal of Lightwave Technology*, vol. 16, no. 7, pp. 1285-1294, July1998.

[3] Nyman, B. M. and Wolter, G., "High-Resolution Measurement of Polarization-Dependent Loss," *Ieee Photonics Technology Letters*, vol. 5, no. 7, pp. 817-818, July1993.

[4] Gisin, N., "Statistics of Polarization-Dependent Losses," *Optics Communications*, vol. 114, no. 5-6, pp. 399-405, Feb.1995.

[5] Collett, E., *Polarized Light, Fundamentals and Applications* New York, NY: Marcel Dekker, Inc., 1993.

[6] R.Ulrich, S.C.Rasleigh, and W.Eickoff, "Bending induced birefringence in single mode fibers," *Optics Letters*, vol. 5 pp. 273-275, 1980.